JACS
JOURNAL OF THE AMERICAN CHEMICAL SOCIETY
Article
pubs.acs.org/JACS

Induction of Chirality in an Achiral Monolayer at the Liquid/Solid Interface by a Supramolecular Chiral Auxiliary

Inge De Cat,[†] Zongxia Guo,[†,§] Subi J. George,[‡] E. W. Meijer,[‡] Albertus P. H. J. Schenning,*[,‡] and Steven De Feyter*[,†]

[†]Department of Chemistry, Division of Molecular Imaging and Photonics, KU Leuven - University of Leuven, Celestijnenlaan 200F, 3001 Leuven, Belgium

[‡]Laboratory of Macromolecular and Organic Chemistry, Eindhoven University of Technology, P.O. Box 513, 5600MB Eindhoven, The Netherlands

Supporting Information

ABSTRACT: An achiral oligo(*p*-phenylene vinylene) derivative with a ureido-triazine hydrogen bonding unit self-assembles into rows of hydrogen bonded dimers at the liquid/solid interface. Scanning tunneling microscopy reveals the formation of chiral domains, but overall, the surface remains racemic. Addition of a chiral auxiliary which is able to interact with the dimers through hydrogen bonding, showed that global organizational chirality could be achieved since a majority of the domains show the same handedness. After removing the chiral auxiliary with a volatile solvent, the global organizational chirality could be trapped, revealing a memory effect. With this straightforward supramolecular approach, we were able to create a chiral surface with preferred handedness composed of achiral molecules at the air/solid interface.

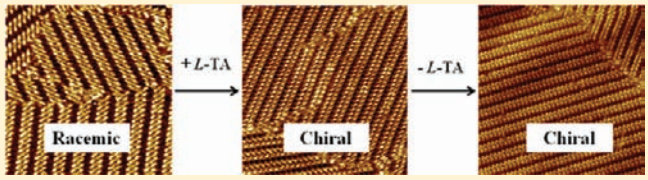

INTRODUCTION

Although chirality has been intensively studied since Pasteur resolved tartaric acid,[1] still many aspects remain to be discovered. In two dimensions, expression of chirality on a surface, studied by scanning tunneling microscopy (STM), has been a focus area for many years.[2−9] Now, the focus has shifted toward induction and amplification of chirality.[10−14] This has led to new and easy methods to create chiral surfaces, which are widely applicable, for example, as enantioselective surfaces.

A variety of studies on crystals have shown that it is possible to form homochiral architectures. Chiral purity can be induced during crystallization by nonlinear autocatalysis and recycling.[15,16] Also absolute asymmetric synthesis in chiral crystals have been achieved.[17,18]

In solution, induction and transfer of chirality has been studied for polymers[19−21] and later for self-assembled systems.[22−26] In these systems, the so-called "sergeants and soldiers principle" has shown to be a successful approach. A small amount of chiral molecules can transfer their chirality to a majority of achiral molecules turning the whole system into homochirality. Remarkably, in self-assembled systems, the sergeant could be replaced or removed resulting in kinetically trapped homochiral assemblies composed of achiral building blocks.[27] Not only sergeants can induce chirality, but also chiral auxiliary molecules, which can interact with the assembly of achiral molecules through noncovalent interactions.[28] In solution, it was reported that by adding a chiral acid to a racemic mixture of helical stacks composed of achiral molecules, the handedness of the helices could be tuned.[29] The chiral acid was able to interact with the achiral molecules through hydrogen bonds and, as a result, was able to transfer its chirality. Similar results were obtained by selective solvation in chiral alcohol−hydrocarbon combinations.[30] Also electrostatic interactions can be used to promote the transformation from racemic to chiral nanostructures.[31,32]

Chirality at the liquid/solid interface can be expressed in different ways: packing of the molecules or the orientation of the monolayer with respect to the underlying substrate. Achiral molecules can form chiral patterns on a surface due to their constraint in two dimensions. The overall surface area stays racemic since both mirror images of the chiral structures are equally present. Global chirality or even homochirality at the surface can be induced when multicomponent structures, consisting of chiral and achiral molecules, are adsorbed together on a surface.[33,34] Recently, it was even reported that global chirality can also be induced in a monolayer of achiral molecules by using a chiral solvent, which does not affect the original supramolecular organization.[35] In this study, we show that only a 10-fold excess of small chiral molecules can have the same effect as a chiral solvent. In fact, our approach to achieve homochiral surfaces is inspired by experiments carried out in solution: a derivate of tartaric acid was used to induce homochirality in stacks of an achiral oligo(*p*-phenylene vinylene) derivative equipped with a ureido-triazine end group (**AOPV3**) (Figure 1A) and this homochirality remained present after removing the tartaric acid with base at low temperatures. Kinetic experiments revealed the kinetic stability

Received: November 13, 2011
Published: February 3, 2012

   dx.doi.org/10.1021/ja2106652 | *J. Am. Chem. Soc.* 2012, 134, 3171−3177

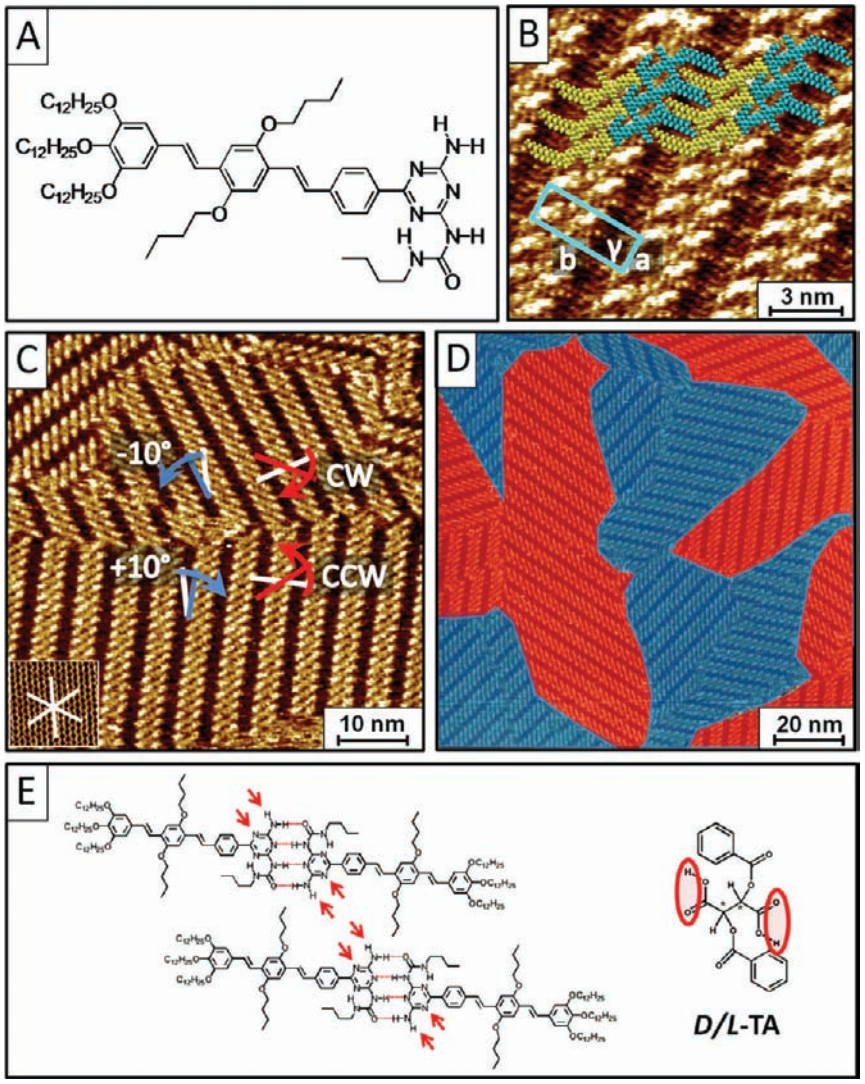

Figure 1. (A) Molecular structure of **AOPV3** (B–D) STM-images of a monolayer of pure **AOPV3** at the TCB/HOPG interface. (B) I_{set} = 45 pA, V_{set} = −860 mV, a model of 6 dimers is superimposed. The **AOPV3** molecules in a dimer are colored yellow and blue. (C) I_{set} = 109 pA, V_{set} = −860 mV, inset: graphite and set of main symmetry axes of graphite <11−20> in white. Blue arrows indicate the angle between a symmetry axis of graphite and the lamella direction. Red arrows show the angle between the normal of the lamella direction and the direction of the dimers. (D) I_{set} = 62 pA, V_{set} = −1040 mV, large scale STM-image with CW domains colored in blue and CCW colored in red. (E) Left: Molecular model of packed **AOPV3** dimers. Red arrows indicate the free hydrogen bonding sites. Right: Molecular structure of chiral handle: ***D/L*-TA**. Red ellipses indicate hydrogen bonding sites.

of the homochiral stacks of achiral molecules.[36] Here, we use a related approach to achieve homochiral surfaces with the same molecules. Note that the experimental conditions are intentionally modified aiming at the formation of 2D surface-confined supramolecular layers rather than the solution-based supramolecular fibers.[36]

By adding dibenzoyl tartaric acid to **AOPV3**, global organizational chirality was induced without drastically changing the packing. Since the number of chiral solvents is limited, using a chiral auxiliary to induce global organizational chirality is more straightforward and will enlarge the range of application possibilities. In addition, the chiral auxiliary can be removed from the surface with a volatile solvent, preserving a memory effect. As a result, the global organizational chirality could be trapped and a chiral monolayer was formed containing exclusively achiral molecules.

■ EXPERIMENTAL DETAILS

STM-experiments were performed on a Molecular Imaging PicoSPM (Agilent). The tips were mechanically cut from Pt/Ir wire (80%/20%, diameter 0.2 mm). The STM-images were obtained in the constant current mode. For analysis, images of the graphite substrate underneath the monolayer were recorded immediately after recording an image of the monolayer. The images were corrected for drift with scanning probe image processor (SPIP) software (Image Metrology ApS) using the recorded graphite images for calibration purposes. The imaging parameters are indicated in the figure captions: tunneling current I_{set} and sample bias V_{set}.

The molecules were dissolved in 1,2,4-trichlorobenzene (TCB) (Sigma-Aldrich >99%) or/and chloroform (Sigma-Aldrich ≥99.8%, ACS spectrophotometric grade). A droplet of the solution was applied onto a freshly cleaved surface of highly oriented pyrolytic graphite (HOPG, grade ZYB, Advanced Ceramics, Inc., Cleveland, OH). To explore the memory effect, ethylene diamine (redistilled, Aldrich ≥99.5%) was used.

dx.doi.org/10.1021/ja2106652 | J. Am. Chem. Soc. 2012, 134, 3171−3177

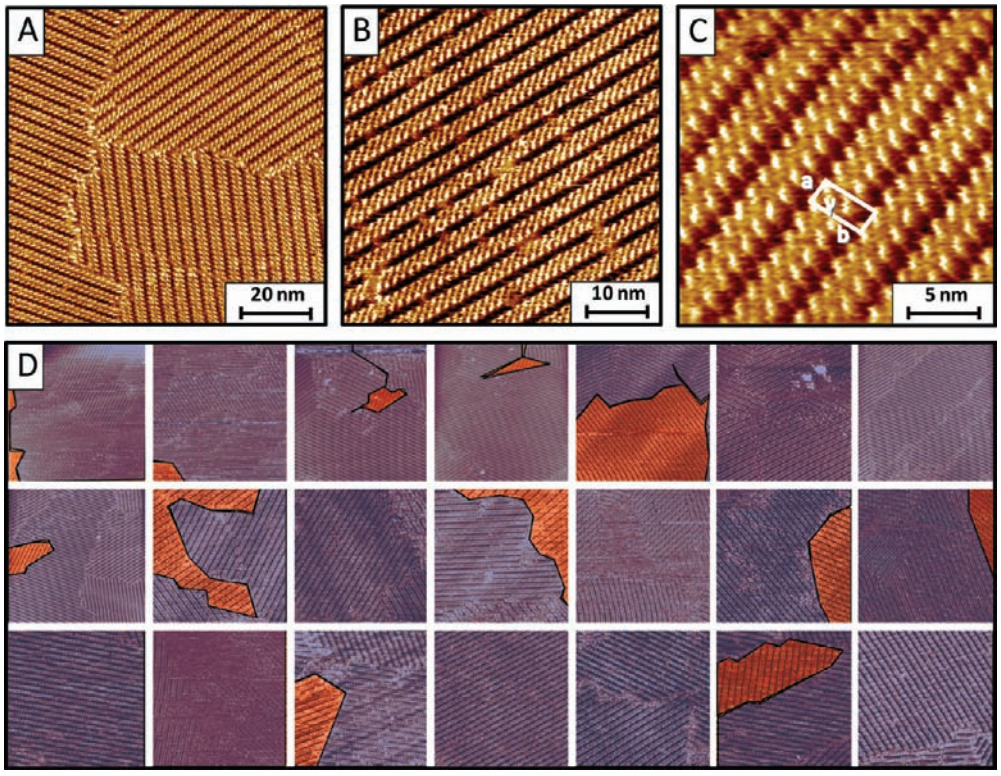

Figure 2. STM-images of a mixture of **AOPV3** and ***D*-TA** at the chloroform−TCB/graphite interface. (A−C) I_{set} = 127 pA, V_{set} = −860 mV with a unit cell shown in C. (D) A selection of analyzed STM-images. The CW domains are colored blue, the CCW domains red. Each image has a size of approximately 100 × 100 nm^2.

For the data analysis, it was necessary to calculate the overall coverage of one type of species. To ensure a high enough resolution, STM-images of approximately 100 nm × 100 nm were collected. To statistically sample the surface, STM-images were recorded on various spots on the graphite. This was done for different samples and on several days to make sure the results are reproducible and give a full account of the samples' heterogeneity. For each image, the exact area of every species was calculated and then the weighted average per session and the overall weighted average and standard deviation were determined. In the Supporting Information, the number of images used is indicated.

■ RESULTS AND DISCUSSION

Oligo(*p*-phenylene vinylene) derivative **AOPV3** equipped with a ureido-triazine end group[37] self-assembles into a densely packed monolayer at the TCB/graphite interface. Two molecules form a dimer due to four hydrogen bonding interactions between the ureido triazine end groups (Figure 1). These dimers stack into lamella, which are packed through two-by-two interdigitation of the long dodecyl chains. Figure 1B shows a high resolution image of the monolayer. The bright rods correspond to the backbone of the OPV-molecules and the darker parts in between the lamella correspond to the alkyl chains. The unit cell parameters are: a = 1.6 ± 0.1 nm, b = 4.6 ± 0.1 nm, and γ = 85 ± 1°. Within an STM-image, mirror domains can be found (Figure 1C). The chirality of the domains can be recognized instantaneously by looking at the angle between the direction of the dimers and the normal of the lamella direction. This angle can be described as clockwise (CW) or counterclockwise (CCW). The direction of the lamella also shows a small angle against a main symmetry axis of graphite <11−20>: −9 ± 3° for the domains with CW dimers and +11 ± 3° for the domains with CCW dimers. Since there are three main symmetry axes of graphite and the orientation of the domains is directed by these axes, three different sets of CW and CCW mirror domains are present. The surface is covered with 47 ± 3% of CW dimers and 53 ± 3% of CCW dimers, so both CW and CCW domains are equally present. A large scale STM-image (Figure 1D) illustrates many small domains. The chirality of the domains is color-coded: blue for CW and red for CCW domains. On average, 16 different domains can be found in an STM-image of 100 × 100 nm^2 and the combined length of the domain boundaries is approximately 569 nm.

Now that the self-assembly and chirality of the monolayer is established, a small chiral molecule that is able to interact with the OPV-molecules can be selected. Figure 1E shows that, when a dimer is formed, there are still some hydrogen bonding sites left: two per molecule, which means two on either side of a dimer. The chiral auxiliary should have four corresponding hydrogen bonding sites, so it can link two dimers and thus have a higher probability to transfer its chirality and stabilize the packing.[32]

A tartaric acid derivative fits the requirements and benzoyl groups were added to increase solubility. (±)-2,3-Dibenzoyl-D/L-tartaric acid (***D*/*L*-TA**), shown in Figure 1E, was used as a supramolecular chiral auxiliary. To ensure that both **AOPV3** and **TA** are molecularly dissolved, chloroform was used as a cosolvent. Chloroform was then mixed with TCB in a 1:10 ratio to create appropriate conditions for STM imaging at the liquid/solid interface. A concentration and ratio dependent study was carried out (Supporting Information Table S1). A maximum in the chiral induction was observed for a heated solution (70°) of a mixture of TCB and chloroform with an excess of the chiral acid molecules (1:10).

dx.doi.org/10.1021/ja2106652 | *J. Am. Chem. Soc.* 2012, 134, 3171−3177

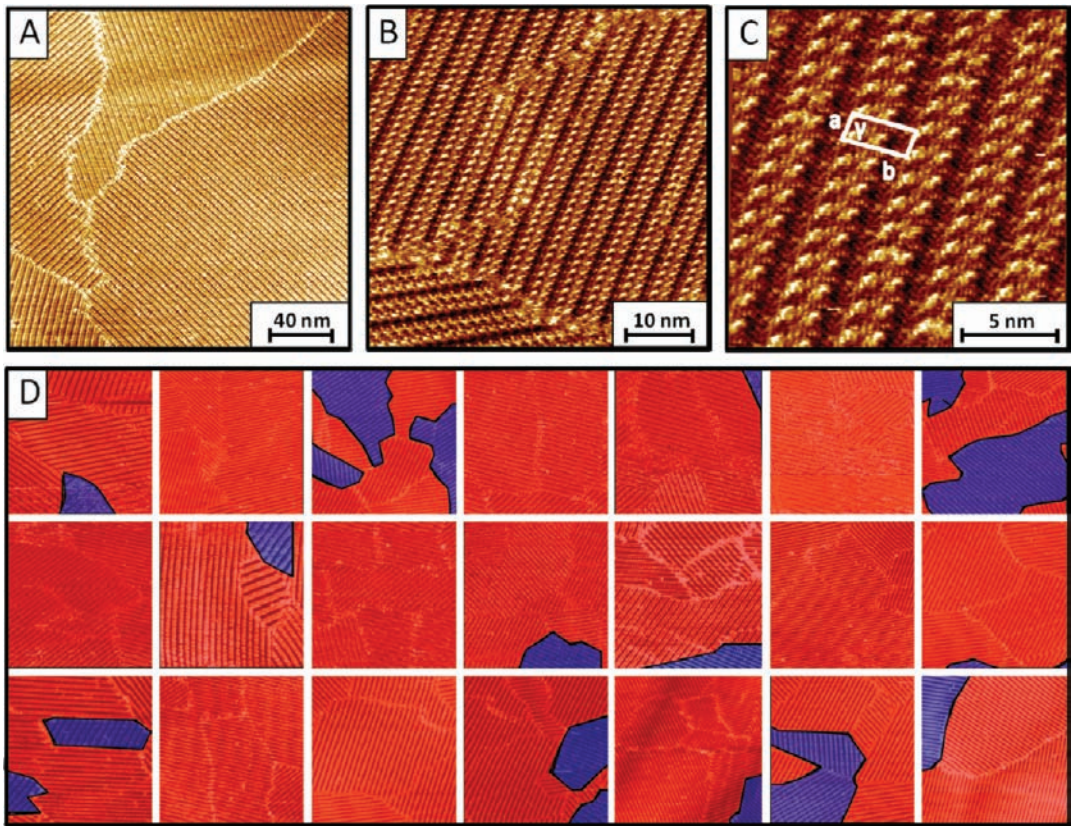

Figure 3. STM-images of a mixture of **AOPV3** and ***D*-TA** at the Chloroform-TCB/graphite interface. (A–C) I_{set} = 33 pA, V_{set} = −860 mV with a unit cell shown in C. (D) A selection of analyzed STM-images. The CW domains are colored blue, the CCW domains red. Each image has a size of approximately 100 × 100 nm^2.

A droplet of the heated premixed solution of **AOPV3** and ***D*-TA** was placed on HOPG and its self-assembly was studied with STM. The STM-images in Figure 2A–C show that domains of dimers are formed which stack into lamella, similar to the self-assembly of pure **AOPV3**. The chiral auxiliary does not appear to be adsorbed on graphite, since the unit cell parameters have not changed significantly: a = 1.6 ± 0.1 nm, b = 4.7 ± 0.1 nm, and γ = 83 ± 2°. The angle between a symmetry axis of graphite and the lamella is −12 ± 3° for CW domains and +9 ± 2° for CCW domains, which is also similar to the results obtained for pure **AOPV3**. The packing has not changed significantly, but the domain size has. The domains are now much larger than for pure **AOPV3**. On average, 5 different domains can be found in an STM-image of 100 × 100 nm^2 with a combined boundary length of 230 nm. The domains are more stable and when we take a closer look at the chirality of the dimers, a large bias to form CW dimers was observed. Figure 2D shows a selection of analyzed STM-images with a size of approximately 100 × 100 nm^2. In each image, the area of CW dimers (shown in blue) and CCW dimers (shown in red) domains was calculated. To quantify the excess, a statistical analysis was carried out (see Experimental Details). As a result, calculations show that 85 ± 8% of the surface is covered with CW dimers, while only 15% of the surface is covered with CCW dimers. The chiral auxiliary clearly influences the chirality of the monolayer by favoring the formation of CW dimers.

For the self-assembly of a mixture of **AOPV3** and ***L*-TA**, similar results were found. The STM-images in Figure 3A–C show that again large domains of stacked dimers are formed. On average, only 4 different domains with a domain boundary length of 241 nm can be found in an image of 100 × 100 nm^2. The unit cell parameters are a = 1.6 ± 0.1 nm, b = 4.7 ± 0.1 nm, and γ = 84 ± 1°. The angle between a symmetry axis of graphite and the lamella is −12 ± 3° for CW domains and +13 ± 3° for CCW domains. Then the STM-images were analyzed in detail as was done for the mixture for **AOPV3** and ***D*-TA**. A selection of these analyzed images is shown in Figure 3D and a bias for CCW dimers can clearly be seen. We found 81 ± 9% of the surface is now covered with CCW dimers. As was expected, the effect of the L-enantiomer on the dimers was opposed to the effect of the D-enantiomer. Thus, by choosing the chirality of the chiral auxiliary, **TA**, the chirality of the monolayer can be tuned.

The previous experiments were carried out with premixed solutions of **AOPV3** and the chiral auxiliary. Now the question arises if sequential addition has the same effect. First, a droplet of pure **AOPV3** is left to self-assemble on the surface, and as previously shown, many small domains are formed with an equal amount of CW and CCW dimers (Supporting Information Figure S1). When a 10-fold excess of ***D*-TA** was added, this ratio changed to 62 ± 4% CW and 38 ± 4% CCW dimers. The domains also stay smaller. In contrast with the premixed solutions, still approximately 11 domains with a combined boundary length of 524 nm are found in an STM-image of 100 × 100 nm^2. The domain size is a little bit larger than for pure **AOPV3** and there is a small bias for one kind of dimers. This means that the chiral auxiliary still influences the chirality, but the preformed achiral monolayer diminishes the effect. The dimers now have to desorb first before they can adsorb with the favored chirality, which is kinetically

dx.doi.org/10.1021/ja2106652 | *J. Am. Chem. Soc.* 2012, 134, 3171–3177

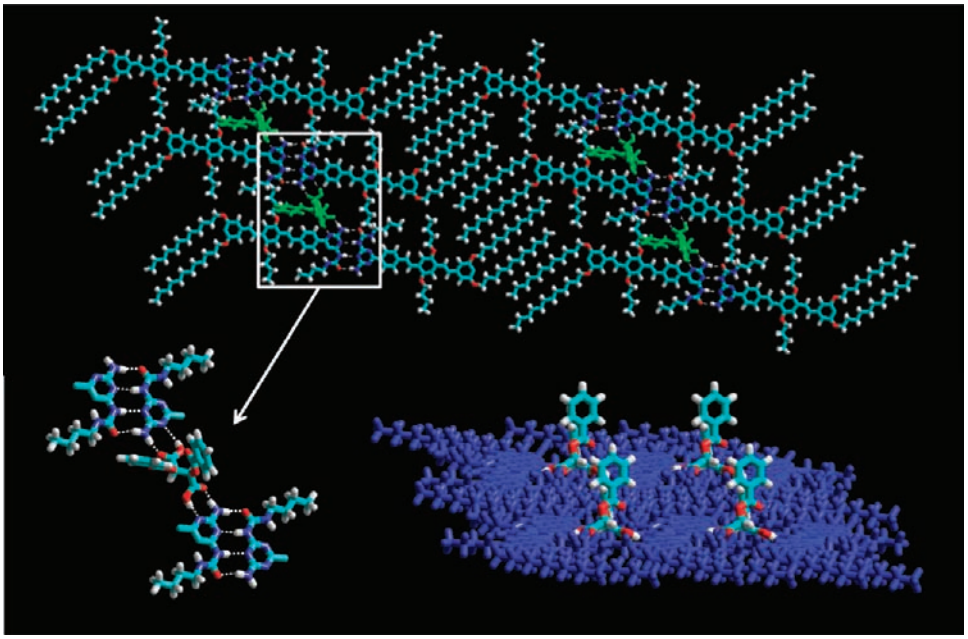

Figure 4. Model of a CW domain of **AOPV3** and ***D*-TA**. Top-view (top) of the model with the chiral auxiliaries shown in green. A close-up (lower left corner) of the hydrogen bonding interactions between both molecules. A side-view of the model (lower right corner) with **AOPV3** shown in dark blue.

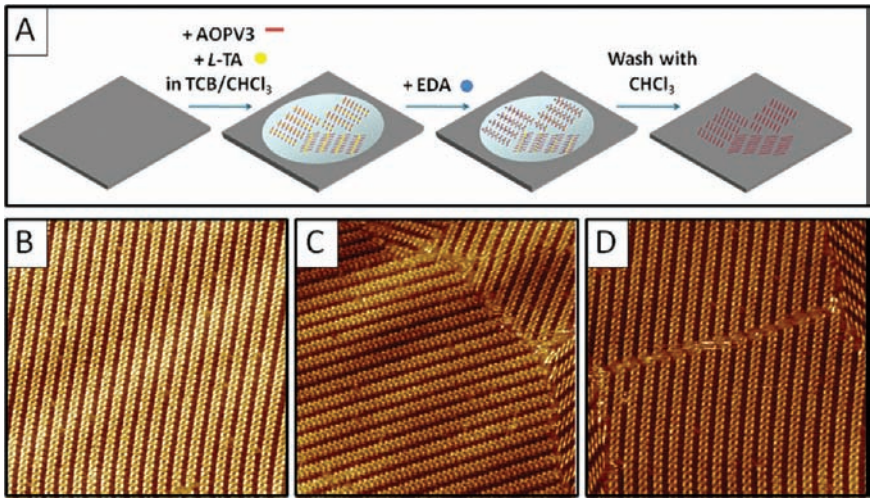

Figure 5. (A) Protocol to remove **TA** from surface with EDA. (B–D) STM-images collected 4 h after washing with $CHCl_3$ with a size of 90.4 × 90.4 nm^2, I_{set} = 109 pA and V_{set} = −860 mV.

unfavorable. This also explains why the domains stay smaller. It takes energy to change the chirality of a preformed stable domain. Therefore, only a small part of the monolayer is able to change and only a small induction effect can be seen, within the time frame of a typical experiment (few hours). In contrast, for the premixed solutions, the dimers can directly adsorb with the preferred chirality and larger domains are able to grow.

To get more insight in the mechanism of the chiral induction, it is necessary to know what happens in solution. Fluorescence measurements were carried out to investigate if there is any complex formation between **AOPV3** and the chiral auxiliary in the premixed solutions, prior to dropcasting on the graphite support. When ***D*-** or ***L*-TA** were added to **AOPV3** in chloroform (Supporting Information Figure S2), or a mixture of chloroform and TCB (Supporting Information Figure S3) under conditions identical to those used for self-assembly at the liquid/solid interface, the fluorescence spectra did not change. In contrast, in a more apolar solvent like methylcyclohexane, a large redshift, quenching of the signal and a change in color was observed (Supporting Information Figure S4).[36] This indicates that, in methylcyclohexane, **AOPV3** and **TA** interact most likely leading to the formation of stacks of hydrogen bonded **AOPV3**/**TA** complexes. For the solvent mixture of chloroform and TCB employed at the liquid/solid interface, there are no indications for complex formation between **AOPV3** and **TA** in solution. This means that graphite plays a crucial role in the interactions between these molecules.

Now, a model of the monolayer surface can be made. In Figure 4, a CW domain of **AOPV3** and ***D*-TA** is shown. For the OPV-molecules, only two of the three dodecyl chains are adsorbed on the surface; the remaining alkyl chain stays in solution. Then, the location and interaction of the chiral

dx.doi.org/10.1021/ja2106652 | *J. Am. Chem. Soc.* 2012, 134, 3171–3177

auxiliaries were examined. Since no significant difference in the unit cell parameters was found and since the chiral molecules could not be visualized with STM, we suggest a model in which the chiral auxiliaries do not interact with the graphite substrate, but are able to interact with the monolayer through hydrogen bonding between two consecutive dimers. Because of these noncovalent interactions, the chiral auxiliaries are able to transfer their chirality to the dimers. For a premixed solution, the presence of the chiral auxiliaries in solution favors the adsorption of one kind of dimer, explaining the large domains and bias. In contrast, when the chiral auxiliary was sequentially added, there was already a stable monolayer present. To have a big induction effect and large domains of a preferred orientation, reorganization is required. Whole domains of molecules have to desorb and adsorb again, which is more difficult. The dimers are kinetically trapped leading to smaller domains and a smaller bias upon sequential addition.

The final step to form a chiral surface containing only achiral molecules is to remove the chiral auxiliary and preserve the memory effect. Ethylene diamine (EDA) is a base, which is able to react with the chiral acid from the surface since it forms a strong acid−base complex with **TA** (Supporting Information Figure S5). To wash the complex away from the surface, a volatile solvent should be chosen since the dynamics present at the liquid/solid interface could destroy the memory effect.[38] At the liquid/solid interface, molecules desorb and adsorb, and after removal of the chiral auxiliaries, there is no driving force for the (re)adsorbing molecules to prefer one specific chirality. This was also proven experimentally with TCB as shown in Supporting Information Figure S6.

When the solvent is very volatile, the rapid evaporation after removal of EDA should trap the organization on the surface and leave a dry surface. The protocol is illustrated in Figure 5A. A heated mixture of **AOPV3** and ***L*-TA** was applied to the surface. Then, an excess of EDA was added and the complex was washed away with chloroform. After 4 h, STM-images were recorded at the air/solid interface. Large domains of stacked dimers could be visualized (Figure 5B−D). On average, 2 domains with a combined domain boundary length of 133 nm were found in an STM-image of 100 × 100 nm^2. To see if this approach has preserved the memory effect, a statistical analysis of the surface coverage was performed. Results showed 75 ± 9% of the surface is covered with CCW dimers and no time dependence was found. The dimers are trapped at the air/solid interface and a lasting memory effect is established. The global organizational chirality of the monolayer is maintained after removing the chiral auxiliary, and therefore, a chiral surface was made out of achiral molecules.

CONCLUSIONS

We showed that chirality with a preferred handedness can be induced in an overall achiral surface by adding a small amount of chiral auxiliary which can interact with the achiral monolayer at the liquid/solid interface. The chiral auxiliary did not influence the original packing but affected the ratio of CW and CCW dimers. While no perfect induction was achieved, about 85% of dimers of a given handedness, defined by the chiral auxiliary, were obtained. When a base was added, the chiral auxiliary could be removed. By choosing a volatile solvent, we were able to kinetically trap the molecules and their global organizational chirality at the air/solid interface. As a result, a chiral surface was formed only composed of achiral molecules and a simple method to create chiral surfaces from achiral molecules was established. These experiments can be connected to what has been achieved in solution.[36] Although the processes of self-assembly at a surface are thought to be different from those in solution, the principles are very much alike and some general guidelines can be constructed.

ASSOCIATED CONTENT

Supporting Information

Solution and ratio dependence of premixed solutions of **AOPV3** and **TA**. STM images after sequential addition. Fluorescence measurements in chloroform, in a mixture of TCB and chloroform and in methylcyclohexane. The complex formed between **TA** and EDA. The loss of a memory effect at the liquid/solid interface when using TCB as the solvent to wash EDA away. This material is available free of charge via the Internet at http://pubs.acs.org.

AUTHOR INFORMATION

Corresponding Author

A.P.H.J.Schenning@tue.nl; Steven.DeFeyter@chem.kuleuven.be

Present Address

[§]Qingdao Institute of Bioenergy and Bioprocess Technology, Chinese Academy of Sciences, Qingdao 266101, China.

Notes

The authors declare no competing financial interest.

ACKNOWLEDGMENTS

We thank Prof. Richard Kellogg (Syncom, Groningen, The Netherlands) for stimulating discussions and for providing the tartaric acid derivative. The research leading to these results has received funding from the European Community's Seventh Framework Program under grant agreement no. NMP4-SL-2008-214340, project RESOLVE. Furthermore, this work is supported by the Fund of Scientific Research − Flanders (FWO), K.U.Leuven (GOA), the Belgian Federal Science Policy Office through IAP-6/27, the Institute for the Promotion of Innovation by Science and Technology in Flanders (IWT), the European Science Foundation (Euryi) and The Netherlands Organization for Scientific Research (NWO).

REFERENCES

(1) Pasteur, L. *Ann. Chim. Phys.* **1848**, *24*, 442−459.
(2) Walba, D. M.; Stevens, F.; Clark, N. A.; Parks, D. C. *Acc. Chem. Res.* **1996**, *29*, 591−597.
(3) Fang, H; B.; Giancarlo, L. C.; Flynn, G. W. *J. Phys. Chem. B* **1998**, *102*, 7311−7315.
(4) Kuhnle, A.; Linderoth, T. R.; Hammer, B.; Besenbacher, F. *Nature* **2002**, *415*, 891−893.
(5) De Feyter, S.; De Schryver, F; C. *Chem. Soc. Rev.* **2003**, *32*, 139−150.
(6) Ernst, K.- H. *Top. Curr. Chem.* **2006**, *265*, 209−252.
(7) Katsonis, N.; Lacaze, E.; Feringa, B. L. *J. Mater. Chem.* **2008**, *18*, 2065−2073.
(8) Raval, R. *Chem. Soc. Rev.* **2009**, 707−721.
(9) Elemans, J. J. A. W.; De Cat, I.; Xu, H.; De Feyter, S. *Chem. Soc. Rev.* **2009**, *38*, 722−736.
(10) Humblot, V; Lorenzo, M. O.; Baddeley, C. J.; Haq, S.; Raval, R. *J. Am. Chem. Soc.* **2004**, *126*, 6460−6469.
(11) Mamdouh, W.; Uji-i, H.; Gesquiere, A.; De Feyter, S.; Amabilino, D. B.; Abdel-Mottaleb, M. M. S.; Veciana, J.; De Schryver, F. C. *Langmuir* **2004**, *20*, 9628−9635.
(12) Berg, A. M.; Patrick, D. L. *Angew. Chem. Int. Ed.* **2005**, *44*, 1821−1823.

(13) Dmitriev, A.; Spillmann, H.; Stepanow, S.; Strunskus, T.; Woll, C.; Seitsonen, A. P.; Lingenfelder, M.; Lin, N.; Barth, J. V.; Kern, K. *ChemPhysChem* **2006**, *7*, 2197−2204.
(14) Ernst, K.- H. *Curr. Opin. Colloid Interface Sci.* **2008**, *13*, 54−59.
(15) Soai, K.; Niwa, S.; Hori, H. *Chem. Commun.* **1990**, 982−983.
(16) Viedma, C. *Phys. Rev. Lett.* **2005**, *94*, 065504.
(17) Penzien, K.; Schmidt, G. M. J. *Angew. Chem., Int. Ed.* **1969**, *8*, 608−609.
(18) Addadi, L.; Lahav, M. *J. Am. Chem. Soc.* **1979**, *101*, 2152−2156.
(19) Green, M. M.; Peterson, N. C.; Sato, T.; Teramoto, A.; Cook, R.; Lifson, S. *Science* **1995**, *268*, 1860−1866.
(20) Yashima, E.; Maeda, K.; Okamoto, Y. *Nature* **1999**, *399*, 449−451.
(21) Green, M. M.; Cheon, K. S.; Yang, S. Y.; Park, J. W.; Swansburg, S.; Liu, W. H. *Acc. Chem. Res.* **2001**, *34*, 672−680.
(22) Palmans, A. R. A.; Vekemans, J. A. J. M.; Havinga, E. E.; Meijer, E. W. *Angew. Chem., Int. Ed.* **1997**, *36*, 2648−2651.
(23) (a) Rivera, J. M.; Craig, S; L.; Martin, T.; Rebek, J. *Angew. Chem., Int. Ed.* **2000**, *39*, 2130. (b) Von Berlepsch, H.; Kirstein, S.; Bottcher, C. *J. Phys. Chem. B* **2003**, *107*, 9646−9654.
(24) (a) Lohr, A.; Würthner, F. *Chem. Commun.* **2008**, *19*, 2227−2229. (b) Isare, B.; Linares, M.; Zargarian, L.; Fermandjian, S.; Miura, M.; Motohashi, S.; Vanthuyne, N.; Lazzaroni, R.; Bouteiller, L. *Chem.—Eur. J.* **2010**, *16*, 173−177.
(25) Toyofuku, K.; Alam, M. A.; Tsuda, A.; Fujita, N.; Sakamoto, S.; Yamaguchi, K.; Aida, T. *Angew. Chem., Int. Ed.* **2007**, *46*, 6476−6480.
(26) Palmans, A. R. A.; Meijer, E. W. *Angew. Chem., Int. Ed.* **2007**, *46*, 8948−8968.
(27) (a) Helmich, F.; Lee, C. C.; Schenning, A. P. H. J.; Meijer, E. W. *J. Am. Chem. Soc.* **2010**, *132*, 16753−16755. (b) Prins, L. J.; De Jong, F.; Timmerman, P.; Reinhoudt, D. N. *Nature* **2000**, *408*, 181−184.
(28) (a) Zhao, J. S.; Ruan, Y. B.; Zhou, R.; Jiang, Y. B. *Chem. Sci.* **2011**, *2*, 937−944. (b) Guo, Z.; De Cat, I.; Van Averbeke, B.; Lin, J.; Wang, G.; Xu, H.; Lazzaroni, R.; Beljonne, D.; Meijer, E. W.; Schenning, A. P. H. J.; De Feyter, S. *J. Am. Chem. Soc.* **2011**, *133*, 17764−17771.
(29) George, S. J.; Tomović, Ž.; Smulders, M. M. J.; de Greef, T. F. A.; Leclère, P. E. L. G.; Meijer, E. W.; Schenning, A. P. H. J. *Angew. Chem., Int. Ed.* **2007**, *46*, 8206−8211.
(30) George, S. J.; Tomović, Ž.; Schenning, A. P. H. J.; Meijer, E. W. *Chem. Commun.* **2011**, *47*, 3451−3453.
(31) Fenniri, H.; Deng, B. L.; Ribbe, A. E. *J. Am. Chem. Soc.* **2002**, *124*, 11064−11072.
(32) Zeng, L. X.; He, Y. J.; Dai, Z. F.; Wang, J.; Cao, Q.; Zhang, Y. L. *ChemPhysChem* **2009**, *10*, 954−962.
(33) De Feyter, S.; Grim, P. C. M.; Rücker, M.; Vanoppen, P.; Meiners, C.; Sieffert, M.; Valiyaveettil, S.; Müllen, K.; De Schryver, F. C. *Angew. Chem., Int. Ed.* **1998**, *37*, 1223−1226.
(34) Qian, P.; Nanjo, H.; Yokoyama, T.; Suzuki, T. M.; Akasaka, K.; Orhui, H. *Chem. Commun.* **2000**, *20*, 2021−2022.
(35) Katsonis, N.; Xu, H.; Haak, R. M.; Kudernac, T.; Tomovíc, Z.; George, S.; Van der Auweraer, M.; Schenning, A. P. H. J.; Meijer, E. W.; Feringa, B. L.; De Feyter, S. *Angew. Chem., Int. Ed.* **2008**, *27*, 4997−5001.
(36) (a) George, S. J.; de Bruijn, R.; Tomović, Ž.; Schenning, A. P. H. J.; Meijer, E. W., manuscript in preparation. (b) Korevaar, P. A.; George, S. J.; Markvoort, A. J.; Smulders, M. M. J.; Hilbers, P. A. J.; Schenning, A. P. H. J.; De Greef, T. F. A.; Meijer, E. W. *Nature* **2012**, *481*, 492−496.
(37) Gesquière, A.; Jonkheijm, P.; Hoeben, F. J. M.; Schenning, A. P. H. J.; De Feyter, S.; De Schryver, F. C.; Meijer, E. W. *Nano Lett.* **2004**, *4*, 1175−1179.
(38) Ciesielski, A.; Lena, S.; Masiero, S.; Spada, G. P.; Samori, P. *Angew. Chem. Int. Ed.* **2010**, *49*, 1963−1966.